crystallization communications

Crystallization and preliminary diffraction analysis of truncated human pleckstrin

Sean Jackson, Seiji Sugiman-Marangos, Kelvin Cheung and Murray Junop*

Department of Biochemistry and Biomedical Sciences, McMaster University, 1200 Main Street West, Hamilton, Ontario L8N 3Z5, Canada

Correspondence e-mail: junopm@mcmaster.ca

Pleckstrin is a major substrate of protein kinase C in platelets and leukocytes and appears to play an important role in exocytosis through a currently unknown mechanism. Pleckstrin function is regulated by phosphorylation, which is thought to cause dissociation of pleckstrin dimers, thereby facilitating phosphoinositide interactions and membrane localization. Evidence also exists suggesting that phosphorylation causes a subtle conformational change in pleckstrin. Structural studies of pleckstrin have been initiated in order to characterize these structural changes and ultimately advance understanding of pleckstrin function. Here, the crystallization and preliminary X-ray diffraction analysis of a truncated version of pleckstrin consisting of the N-terminal PH domain, the protein kinase C phosphorylation sites and the DEP domain (NPHDEP) are reported. In addition, the oligomeric state and phospholipid-binding properties of NPHDEP were analyzed. This work demonstrates that NPHDEP behaves as a monomer in solution and suggests that all three pleckstrin domains contribute to the dimerization interface. Furthermore, based on the binding properties of NPHDEP, the C-terminal PH domain appears to increase the specificity of pleckstrin for phosphoinositides. This work represents a significant step towards determining the structure of pleckstrin.

1. Introduction

Pleckstrin is a major substrate of protein kinase C (PKC) in platelets and leukocytes, where it is expressed at high levels (Lyons *et al.*, 1975; Gailani *et al.*, 1990). Pleckstrin is a modular protein that consists of three domains of approximately equal size (100 residues). The domain architecture includes N-terminal and C-terminal PH (pleckstrin homology) domains separated by a central DEP (dishevelled/EGL10/pleckstrin) domain (Tyers *et al.*, 1989). Both the N-terminal and C-terminal PH (NPH and CPH, respectively) domains have been shown to mediate interactions with phosphoinositides, inositol phosphates and other proteins (Baig, Bao & Haslam, 2009; Baig, Bao, Wolf *et al.*, 2009; Edlich *et al.*, 2005; Abrams, Zhao *et al.*, 1996; Jackson *et al.*, 2007; Harlan *et al.*, 1995; Zhang, 2005). PKC phosphorylates three residues (Ser113, Thr114 and Ser117) that are located on a loop joining the NPH domain and the DEP domain (Abrams, Zhao *et al.*, 1995; Craig & Harley, 1996). Having no known enzymatic activity, pleckstrin appears to function as an adaptor or as a scaffolding protein. Recent studies have provided evidence supporting a role for pleckstrin in exocytosis, although its mechanism of action remains unknown (Ding *et al.*, 2007; Lian *et al.*, 2009).

Phosphorylation regulates pleckstrin activity through a mechanism that appears to alter the oligomeric state and conformation of pleckstrin. Chemical cross-linking studies using both platelet lysate and electropermeabilized platelets showed that pleckstrin could be cross-linked to yield species of higher molecular weight (McDermott & Haslam, 1996). These species corresponded to pleckstrin dimers and higher oligomers. When PKC was activated by PMA prior to cross-linking there was a reduction in the amount of cross-linked species formed (McDermott & Haslam, 1996).
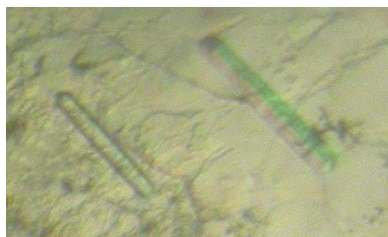
In addition to a change in oligomeric state, evidence for a subtle conformation change as a consequence of phosphorylation has also been provided. Evidence for this stems from the development of a fluorescent probe based on pleckstrin that is designed to detect PKC phosphorylation events. Additional evidence is cited as observed electrophoretic mobility shifts between native and phosphorylated pleckstrin on SDS–PAGE (Brumbaugh, Schleifenbaum, Gasch *et al.*, 2006; Brumbaugh, Schleifenbaum, Stier *et al.*, 2006; Brumell *et al.*, 1997, 1999; Schleifenbaum *et al.*, 2004). How these structural changes affect the overall function of pleckstrin in exocytosis is currently unknown.

To explore these possibilities and to characterize the structural changes resulting from phosphorylation, we have actively pursued crystal structures of full-length native, pseudophosphorylated and dimeric pleckstrin. Here, we report the crystallization and preliminary X-ray diffraction analysis of the first two domains of pleckstrin (NPHDEP). In addition, we describe the oligomeric state and phosphoinositide-binding properties of NPHDEP.

2. Materials and methods

2.1. Expression and purification of pleckstrin proteins

The CPH domain (CPH) was expressed and purified as described previously (Jackson *et al.*, 2007). A construct encoding the NPH and DEP domains (residues 6–229) of human pleckstrin (NPHDEP) was cloned into the pDEST17 expression vector (Invitrogen). NPHDEP was expressed and purified as a hexahistidine-fusion protein in *Escherichia coli* BL21 (DE3). Bacteria were grown in standard LB medium supplemented with 10 mg ml^{-1} ampicillin at 310 K with shaking (225 rev min^{-1}) until the absorbance at 600 nm reached 0.5. Protein expression was induced using 1.0 mM IPTG and the incubation temperature was lowered to 293 K. After a 5 h induction period, the bacteria were harvested by centrifugation at 3315g for 10 min at 277 K. Each 1 l pellet was then resuspended in 8 ml 1× phosphate-buffered saline (PBS) and centrifuged at 3315g for 10 min at 277 K. The resulting cell pellets were flash-frozen in liquid nitrogen and stored at 193 K. Prior to lysis using a French press, pellets (2 l) were resuspended in a final volume of 35 ml nickel *A* buffer (20 mM Tris–HCl pH 7.5, 1.5 M KCl, 0.06% LDAO and 5 mM imidazole). After lysis, the samples were subjected to centrifugation at 48 384g for 40 min at 277 K and the supernatants were applied onto a HiTrap nickel-affinity column (GE Healthcare). The bound proteins were eluted using 300 mM imidazole following sequential washes with 5 and 15 mM imidazole, which was accomplished by mixing appropriate volumes of nickel *A* buffer and nickel *B* buffer (20 mM Tris–HCl pH 7.5, 1.5 M KCl, 0.06% LDAO and 300 mM imidazole). After incubation with 50 mM EDTA for 60 min at 277 K to remove trace amounts of Ni^{2+}, the protein was buffer-exchanged into 20 mM Tris–HCl pH 7.5 and 200 mM KCl using a HiPrep 26/10 desalting column (GE Healthcare). Despite the protein containing a TEV cleavage site for the removal of the N-terminal hexahistidine tag, attempts to do so were unsuccessful. Therefore, all NPHDEP constructs used in this study contained six histidine residues followed by a linker region (DYDIPTT) and a TEV cleavage site (ENLYFQG) N-terminal to the first residue of NPH. The sample was applied onto a HiTrap SP Sepharose HP ion-exchange column (GE Healthcare) to further purify the protein from any remaining contaminants. The protein of interest was subsequently eluted using a salt gradient generated by mixing buffers S-*A* (20 mM Tris–HCl 7.5) and S-*B* (20 mM Tris–HCl 7.5 and 1 M KCl). The final protein samples were buffer-exchanged into experiment-specific buffers (see below) and concentrated using ultrafiltration (GE Healthcare). Protein purity was consistently greater than 95% as determined by SDS–PAGE analysis.

2.2. Gel-filtration analysis

All gel-filtration experiments were performed using a Superdex 200 10/300 GL gel-filtration column (Amersham Biosciences). Low-molecular-weight and high-molecular-weight protein standards (Amersham Biosciences) were used to calibrate the column. The apparent molecular weights of the pleckstrin protein samples were calculated based on the standard curve of protein standards (see Fig. S1[1]). The column was equilibrated with at least ten column volumes of sample buffer (20 mM Tris–HCl pH 7.5, 200 mM KCl and 2 mM TCEP) prior to sample application. Protein samples were diluted in sample buffer. All samples were injected at a flow rate of 0.1 ml min^{-1}. Following sample injection, the flow rate was adjusted to 0.5 ml min^{-1} for the duration of the experiment. All experiments were conducted at 277 K.

2.3. Protein–lipid overlay assays

All protein–lipid overlay assays were performed using PIP Strip membranes from Echelon Biosciences Inc. The membranes were blocked with PBS + 1% nonfat dry milk for 1 h at 294 K prior to incubation with the protein of interest at a concentration of 9.0×10^{-2} μM in sample buffer (20 mM Tris–HCl pH 7.5 and 150 mM KCl) with gentle agitation at 294 K for 1 h. After discarding the protein solution, the membranes were washed twice with 15 ml wash buffer (20 mM Tris–HCl pH 7.5, 150 mM KCl and 1% Tween-20) with agitation at 294 K for 15 min each. The membranes were then incubated for 1 h at 294 K with either anti-pleckstrin (Abnova) or anti-hexahistidine (Invitrogen) mouse monoclonal antibody diluted 1:3500 in sample buffer. The primary antibody was discarded and the membranes were washed as described above. The membranes were then incubated for 1 h at 294 K with alkaline phosphatase-coupled secondary antibody (Bio-Rad) diluted 1:3300 in sample buffer. The membranes were then washed and incubated in 10 ml developing solution (Bio-Rad) for 15 min. The membranes were then rinsed with water, air-dried and scanned using a standard desktop computer scanner.

2.4. Crystallization and data collection

NPHDEP was crystallized using the hanging-drop vapour-diffusion method. A 1.0 μl sample of NPHDEP at 15 mg ml^{-1} in 20 mM Tris–HCl pH 7.5, 200 mM KCl and 2 mM TCEP was mixed with 1.0 μl 0.1 M sodium acetate pH 4.6, 0.2 M ammonium sulfate and 25%(w/v) PEG 4000 and suspended over 500 μl 1.5 M ammonium sulfate. After a three-week incubation at 293 K, crystals possessing a hexagonal rod morphology were observed. A single data set (2.4 Å resolution) was collected at a wavelength of 0.9797 Å on beamline X25 of Brookhaven National Laboratory using an ADSC Q315 CCD area detector. The data were processed using the *d**TREK program suite (Pflugrath, 1999). Molecular replacement was performed using *Phaser* as part of the *PHENIX* program suite (Adams *et al.*, 2002; McCoy *et al.*, 2007).

[1] Supplementary material has been deposited in the IUCr electronic archive (Reference: PU5307).

crystallization communications

3. Results and discussion

3.1. All three pleckstrin domains appear to contribute to dimerization

Chemical cross-linking studies utilizing platelet lysate, electro-permeabilized platelets and purified pleckstrin have shown that pleckstrin self-associates to form dimers (McDermott & Haslam, 1996). In support of this, we have shown that purified recombinant pleckstrin self-associates to form dimers using analytical ultra-centrifugation (manuscript in publication). Previous studies of individual NPH and DEP domains demonstrated that these domains
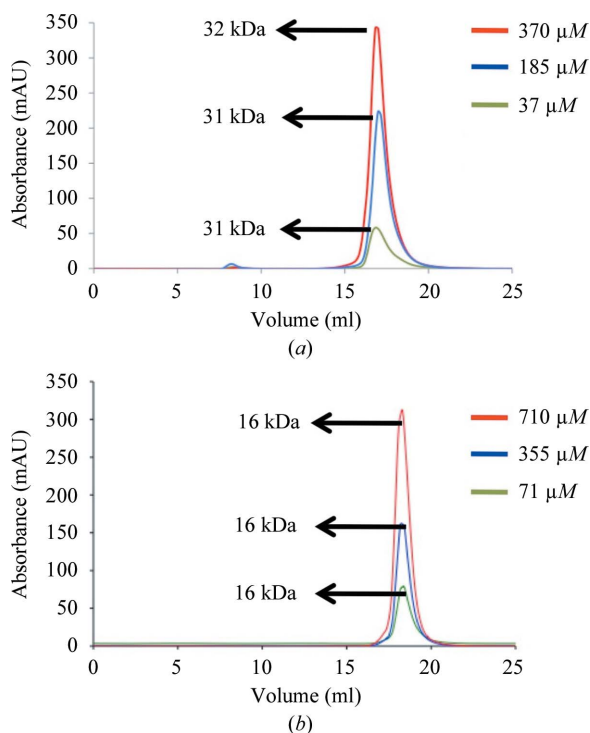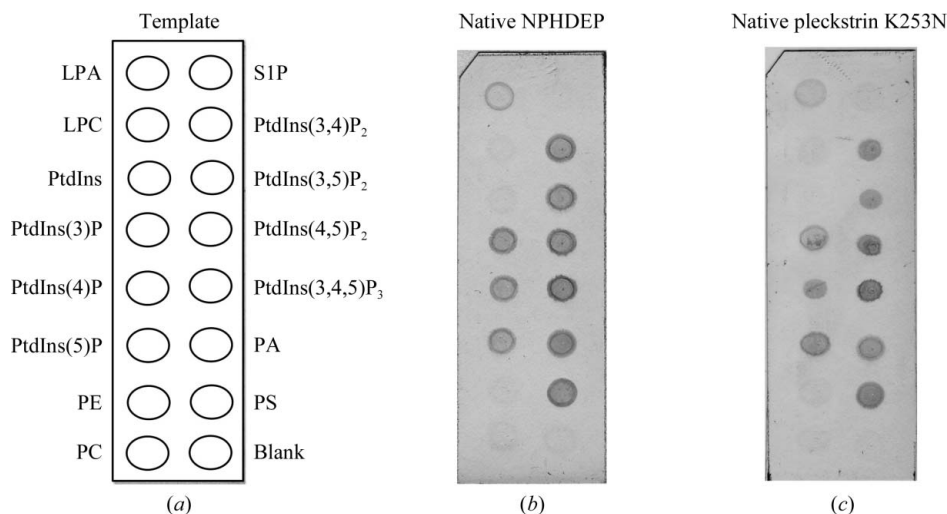

behave as monomers (Yoon *et al.*, 1994; Civera *et al.*, 2005). In order to determine whether NPHDEP alone is sufficient for dimerization, we analyzed its oligomeric state by gel filtration. NPHDEP was analyzed using a concentration range of 37–370 µ*M* (Fig. 1*a*). At these concentrations, NPHDEP eluted with an apparent molecular weight of 31–32 kDa. This suggests that NPHDEP does not self-associate, since the theoretical molecular weight of the NPHDEP construct is approximately 28 kDa. The major difference between NPHDEP and full-length native pleckstrin is the presence of CPH, which therefore suggests that CPH plays an important role in self-association. When CPH (14 kDa) was tested the apparent molecular weight was consistently found to be 16 kDa (Fig. 1*b*). This indicates that like NPH, DEP and NPHDEP, CPH does not self-associate. Therefore, it appears that all three individual domains (NPH, DEP and CPH) contribute significantly to the dimerization interface. Here, the self-association of individual domains or a combination of two domains would be too weak to detect by gel filtration.

3.2. Phospholipid-binding properties of NPHDEP

The phospholipid-binding properties of NPHDEP were examined using protein–lipid overlay assays. NPHDEP bound rather promiscuously to all negatively charged phospholipids (Fig. 2*b*). These results are consistent with a previous study in which NPH was shown to bind with low specificity to negatively charged phospholipids (Kavran *et al.*, 1998). These findings also suggest that DEP does not affect the binding properties of NPH. This contradicts a claim that DEP blocks the NPH binding site, thereby preventing lipid–inositol phosphate interactions (Civera *et al.*, 2005). It is possible that the binding properties of NPHDEP could differ in the context of full-length pleckstrin. To investigate this, we tested the binding properties of a pleckstrin point mutant. The lysine at position 253, which has been shown to be important for phosphoinositide binding (Edlich *et al.*, 2005), was mutated to asparagine (K253N). This mutant displayed the same binding properties as NPHDEP (Fig. 2*c*), suggesting that NPH is capable of phospholipid binding in the context of NPHDEP and full-length pleckstrin. How phosphorylation might affect phospholipid binding is an area of active study in our laboratory and structural information on pleckstrin would be invaluable in understanding how the individual domains contribute to the overall binding properties of pleckstrin.

Figure 1
Gel-filtration analysis of NPHDEP (*a*) and CPH (*b*). The experiments were performed on a calibrated S200 gel-filtration column. The absorbance was monitored at 280 nm. The reported apparent molecular weights were calculated from a standard curve as shown in Fig. S1.

Figure 2
Protein–lipid overlay assays of various pleckstrin proteins. (*a*) shows a schematic diagram of a PIP strip. (*b*) and (*c*) contain NPHDEP and pleckstrin K253N, respectively. Each spot contains 100 pmol of lipid. LPA, lysophosphatidic acid; S1P, sphingosine-1-phosphate; LPC, lysophosphocholine; PE, phosphatidylethanolamine; PC, phosphatidylcholine; PA, phosphatidic acid; PS, phosphatidylserine; PtdIns, phophatidylinositol (with numbers in parentheses indicating the positions of phosphate groups).

Table 1
X-ray data-collection statistics.

Values in parentheses are for the highest resolution shell.

Space group	$P6$
Unit-cell parameters (Å, °)	$a = 71.7$, $b = 71.7$, $c = 70.3$,
	$\alpha = \beta = 90$, $\gamma = 120$
No. of molecules in asymmetric unit	1
Resolution range (Å)	46.51–2.30 (2.38–2.30)
Unique reflections	9158
Data multiplicity	10.8 (10.4)
Completeness (%)	99.8 (99.2)
$\langle I/\sigma(I)\rangle$	15.7 (4.7)
R_{merge} (%)	9.2 (31.7)

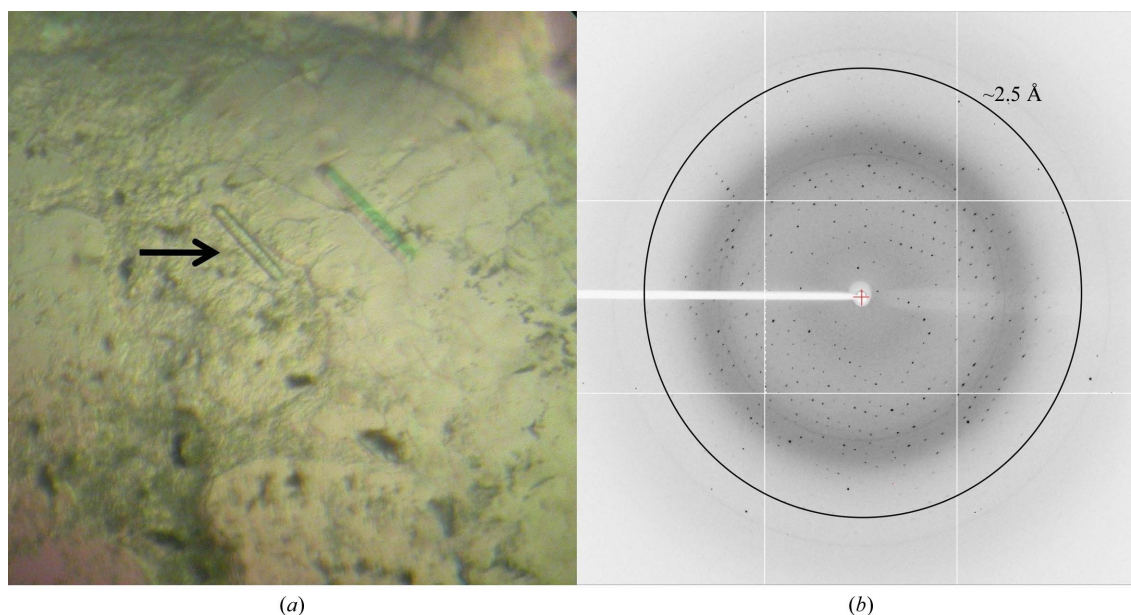### 3.3. X-ray diffraction analysis of NPHDEP crystals

While structural information on full-length pleckstrin would be ideal, the information obtained from the structure of NPHDEP is still very valuable. NPHDEP contains the residues phosphorylated by PKC and the observed conformational change is likely to involve a change in the relative positions of NPH and DEP (Brumbaugh, Schleifenbaum, Gasch *et al.*, 2006; Brumbaugh, Schleifenbaum, Stier *et al.*, 2006; Schleifenbaum *et al.*, 2004). The crystals of NPHDEP possessed a hexagonal rod morphology and grew to maximum size after approximately three weeks (Fig. 3*a*). The NPHDEP crystals diffracted X-rays to beyond 2.5 Å resolution (Fig. 3*b*) and a single native data set was collected. Analysis of the diffraction-pattern symmetry and the systematic absences revealed that the crystals belonged to space group $P6$, with unit-cell parameters a = 71.7, b = 71.7, c = 70.3 Å, α = 90.0, β = 90.0, γ = 120.0°. Data-collection and processing statistics are shown in Table 1. According to the Matthews coefficient calculation there is a single NPHDEP molecule (V_M = 2.1 Å^3 Da^{-1}) in the asymmetric unit. This is consistent with our gel-filtration analysis, which shows that NPHDEP behaves as a monomer in solution.

Since the structures of NPH and DEP have been solved previously by NMR (PDB codes 1pls and 1w4m, respectively; Yoon *et al.*, 1994; Civera *et al.*, 2005), we tried to solve the structure using molecular replacement. Initial molecular-replacement experiments involved search models consisting of the entire NPH and DEP structures as

reported in PDB files 1pls and 1w4m, respectively, with the exception being that all H atoms were removed. Experiments using these search models with varying protocols were unsuccessful. Subsequent experiments involving modified search models in which residues from loop regions in both NPH and DEP were excluded were also unsuccessful, as were experiments involving alternative PH domains as search models. It is possible that the loop region joining NPH and DEP was cleaved by a contaminating protease and that either NPH or DEP crystallized independently. To test for this, control molecular-replacement experiments were performed using NPH and DEP independently as search models. This experiment did not yield a solution, suggesting that NPH or DEP alone had not crystallized.

The success of molecular replacement depends on two primary factors: the quality of the data and the quality of the search model. The X-ray diffraction data are of high quality and present no obvious problems for solution by molecular replacement. This leaves the search model as the most probable cause of the difficulties encountered. Molecular replacement is able to solve structures of unknown proteins by using phase information from a structurally similar protein as an initial estimate for the phase information of the unknown protein. The success of molecular replacement hinges on the accuracy of the initial phase estimate, which is directly related to the similarity between the unknown structure and the search model.

Here, the unknown structure is composed of NPH and DEP separated by an intervening loop, corresponding to residues 6–229 of pleckstrin. In addition, there is an N-terminal hexahistidine fusion tag. The structures of NPH and DEP solved previously encompass residues 1–107 and 121–223, respectively, and account for a significant portion of NPHDEP. This being the case, using these structures as search models should in theory be sufficient to provide a molecular-replacement solution. It is possible that NPH and DEP interact in a manner that alters their individual tertiary structures. These alterations could result in differences between the search models and NPHDEP, thereby decreasing the likelihood of success using molecular replacement. NMR analysis of DEP revealed mobility in several regions that could also adversely affect the chances of success using molecular replacement (Civera *et al.*, 2005). Increased mobility is problematic for molecular replacement as it decreases the structural

(a)   *(b)*

Figure 3
X-ray diffraction analysis of NPHDEP. A crystal of NPHDEP is shown in (*a*). These crystals diffracted to beyond 2.5 Å resolution as shown in (*b*).

similarity between the search model and the unknown structure even if the sequence similarity is very high.

In order to circumvent the problems encountered using molecular replacement, the alternative technique of single-wavelength anomalous diffraction is being pursued. In addition, we are creating pseudophosphorylated NPHDEP in which the residues phosphorylated by PKC are mutated to glutamic acids (S113E, T114E and S117E). This strategy has successfully been applied to full-length pleckstrin, where it accurately mimics phosphorylation (Abrams, Wu *et al.*, 1995; Abrams, Zhang *et al.*, 1996; Auethavekiat *et al.*, 1997; Ma & Abrams, 1999; Ma *et al.*, 1997). A structural comparison of NPHDEP and pseudophosphorylated NPHDEP would provide valuable information regarding the observed conformational change.

References

Abrams, C. S., Wu, H., Zhao, W., Belmonte, E., White, D. & Brass, L. F. (1995). *J. Biol. Chem.* **270**, 14485–14492.
Abrams, C. S., Zhang, J., Downes, C. P., Tang, X., Zhao, W. & Rittenhouse, S. E. (1996). *J. Biol. Chem.* **271**, 25192–25197.
Abrams, C. S., Zhao, W., Belmonte, E. & Brass, L. F. (1995). *J. Biol. Chem.* **270**, 23317–23321.
Abrams, C. S., Zhao, W. & Brass, L. F. (1996). *Biochim. Biophys. Acta*, **1314**, 233–238.
Adams, P. D., Grosse-Kunstleve, R. W., Hung, L.-W., Ioerger, T. R., McCoy, A. J., Moriarty, N. W., Read, R. J., Sacchettini, J. C., Sauter, N. K. & Terwilliger, T. C. (2002). *Acta Cryst.* D**58**, 1948–1954.
Auethavekiat, V., Abrams, C. S. & Majerus, P. W. (1997). *J. Biol. Chem.* **272**, 1786–1790.
Baig, A., Bao, X. & Haslam, R. (2009). *Proteomics*, **9**, 4254–4258.
Baig, A., Bao, X., Wolf, M. & Haslam, R. (2009). *Platelets*, **20**, 446–457.
Brumbaugh, J., Schleifenbaum, A., Gasch, A., Sattler, M. & Schultz, C. (2006). *J. Am. Chem. Soc.* **128**, 24–25.
Brumbaugh, J., Schleifenbaum, A., Stier, G., Sattler, M. & Schultz, C. (2006). *Nature Protoc.* **1**, 1044–1055.
Brumell, J. H., Craig, K. L., Ferguson, D., Tyers, M. & Grinstein, S. (1997). *J. Immunol.* **158**, 4862–4871.
Brumell, J. H., Howard, J. C., Craig, K., Grinstein, S., Schreiber, A. D. & Tyers, M. (1999). *J. Immunol.* **163**, 3388–3395.
Civera, C., Simon, B., Stier, G., Sattler, M. & Macias, M. J. (2005). *Proteins*, **58**, 354–366.
Craig, K. L. & Harley, C. B. (1996). *Biochem. J.* **314**, 937–942.
Ding, Y., Kantarci, A., Badwey, J. A., Hasturk, H., Malabanan, A. & Van Dyke, T. E. (2007). *J. Immunol.* **179**, 647–654.
Edlich, C., Stier, G., Simon, B., Sattler, M. & Muhle-Goll, C. (2005). *Structure*, **13**, 277–286.
Gailani, D., Fisher, T. C., Mills, D. C. & Macfarlane, D. E. (1990). *Br. J. Haematol.* **74**, 192–202.
Harlan, J. E., Yoon, H. S., Hajduk, P. J. & Fesik, S. W. (1995). *Biochemistry*, **34**, 9859–9864.
Jackson, S. G., Zhang, Y., Haslam, R. J. & Junop, M. S. (2007). *BMC Struct. Biol.* **7**, 80.
Kavran, J. M., Klein, D. E., Lee, A., Falasca, M., Isakoff, S. J., Skyolnik, E. Y. & Lemmon, M. A. (1998). *J. Biol. Chem.* **273**, 30497–30508.
Lian, L., Wang, Y., Flick, M., Choi, J., Scott, E. W., Degen, J., Lemmon, M. A. & Abrams, C. (2009). *Blood*, **113**, 3577–3584.
Lyons, R. M., Stanford, N. & Majerus, P. W. (1975). *J. Clin. Invest.* **56**, 924–936.
Ma, A. D. & Abrams, C. S. (1999). *J. Biol. Chem.* **274**, 28730–28735.
Ma, A. D., Brass, L. F. & Abrams, C. S. (1997). *J. Cell Biol.* **136**, 1071–1079.
McCoy, A. J., Grosse-Kunstleve, R. W., Adams, P. D., Winn, M. D., Storoni, L. C. & Read, R. J. (2007). *J. Appl. Cryst.* **40**, 658–674.
McDermott, A. M. & Haslam, R. J. (1996). *Biochem. J.* **317**, 119–124.
Pflugrath, J. W. (1999). *Acta Cryst.* D**55**, 1718–1725.
Schleifenbaum, A., Stier, G., Gasch, A., Sattler, M. & Schultz, C. (2004). *J. Am. Chem. Soc.* **126**, 11786–11787.
Tyers, M., Haslam, R. J., Rachubinski, R. A. & Harley, C. B. (1989). *J. Cell. Biochem.* **40**, 133–145.
Yoon, H. S., Hajduk, P. J., Petros, A. M., Olejniczak, E. T., Meadows, R. P. & Fesik, S. W. (1994). *Nature (London)*, **369**, 672–675.
Zhang, Y. (2005). PhD thesis. Department of Medical Sciences, McMaster University, Canada.